Journal of Hydrology 208 (1998) 223–236

Estimating formation properties from early-time recovery in wells subject to turbulent head losses

Allen M. Shapiro[a,*], Delwyn S. Oki[b], Earl A. Greene[c]

[a]US Geological Survey, 431 National Center, Reston, VA 20192, USA
[b]US Geological Survey, 677 Ala Moana Boulevard, Honolulu, HI 96813, USA
[c]US Geological Survey, 8987 Yellow Brick Road, Baltimore, MD 21237, USA

Received 5 August 1997; accepted 13 May 1998

Abstract

A mathematical model is developed to interpret the early-time recovering water level following the termination of pumping in wells subject to turbulent head losses. The model assumes that turbulent head losses dissipate immediately when pumping ends. In wells subject to both borehole storage and turbulent head losses, the early-time recovery exhibits a slope equal to 1/2 on log–log plots of the recovery versus time. This half-slope response should not be confused with the half-slope response associated with a linear flow regime during aquifer tests. The presence of a borehole skin due to formation damage or stimulation around the pumped well alters the early-time recovery in wells subject to turbulent head losses and gives the appearance of borehole storage, where the recovery exhibits a unit slope on log–log plots of recovery versus time. Type curves can be used to estimate the formation storativity from the early-time recovery data. In wells that are suspected of having formation damage or stimulation, the type curves can be used to estimate the 'effective' radius of the pumped well, if an estimate of the formation storativity is available from observation wells or other information. Type curves for a homogeneous and isotropic dual-porosity aquifer are developed and applied to estimate formation properties and the effect of formation stimulation from a single-well test conducted in the Madison limestone near Rapid City, South Dakota. Published by Elsevier Science B.V.

Keywords: Ground water; Pump tests; Turbulence; Transmissivity; Storage coefficient; Madison aquifer

1. Introduction

Estimating formation properties from single-well tests requires knowledge of turbulent head losses in the pumped well so that drawdown in the formation can be separated from head losses associated with the pump operation. Turbulent head losses are identified from step-drawdown tests, in which the head loss attributed to the pump operation is assumed to be proportional to the pumping rate raised to a power greater than one (Jacob, 1947; Rorabaugh, 1953). A common approach to estimating formation properties from single-well tests is to assume that turbulent head losses become constant with time early in the aquifer test. Thus, turbulent head losses for a given pumping rate are subtracted from the measured drawdown in the pumped well, and the late-time drawdown is used to estimate formation properties. For example, in a confined and homogeneous aquifer of infinite areal extent, Jacob (1947) showed that a plot of drawdown versus the logarithm of time yields a straight-line,

* Corresponding author. Fax: +1 703 6485274; e-mail: ashapiro@usgs.gov

0022-1694/98/$ - see front matter. Published by Elsevier Science B.V.
PII S0022-1694(98)00170-X

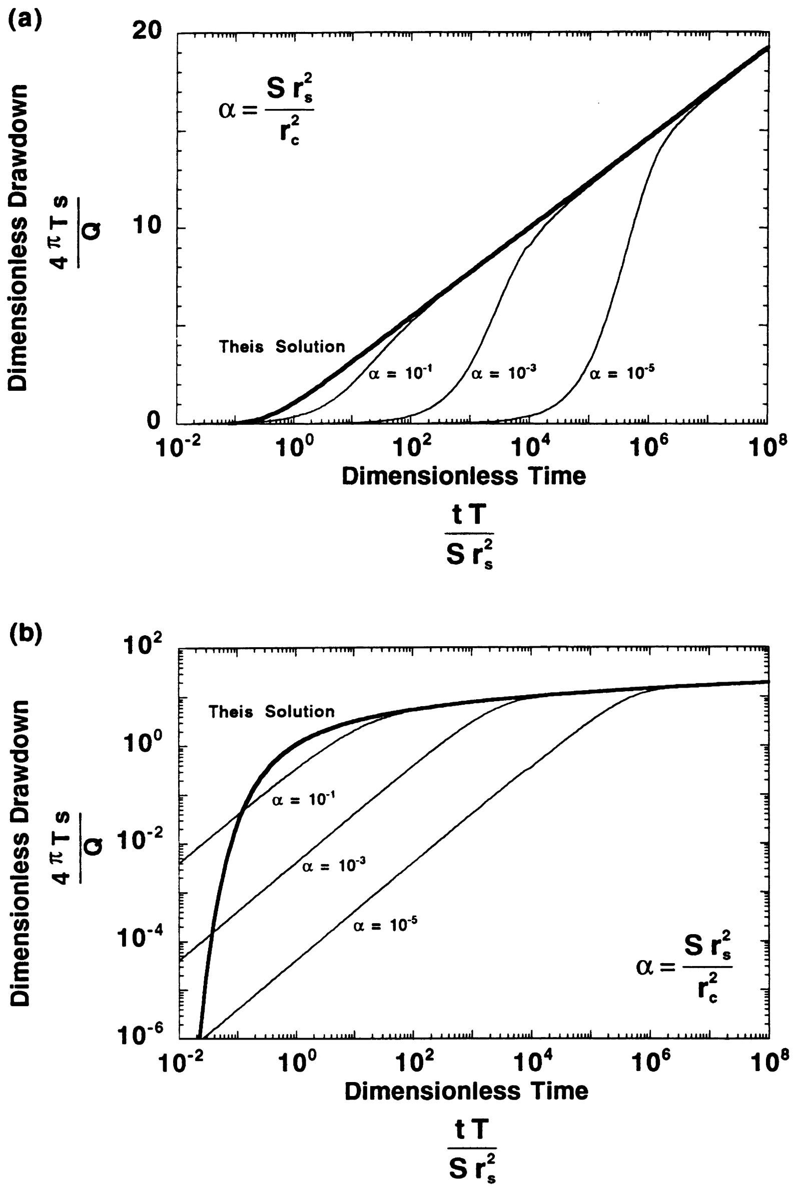

Fig. 1. (a) Drawdown in a finite-diameter borehole versus the logarithm of time, and (b) the logarithm of drawdown in a finite-diameter borehole versus the logarithm of time for values of the dimensionless storage coefficient, α.

with a slope that is inversely proportional to transmissivity. Furthermore, the formation storativity is determined from the intercept of the straight line (corrected for turbulent head losses) at zero drawdown (Jacob, 1947).

In less-permeable formations, borehole storage becomes a factor in analyzing drawdown from single-well tests, and the straight-line approximation for estimating storativity on semilogarithmic plots of drawdown versus time is no longer accurate. For example, Fig. 1a shows semilogarithmic plots of dimensionless drawdown in a finite diameter well versus dimensionless time for different values of the dimensionless storage coefficient. The late-time straight-line response is the same for each solution which would erroneously yield the same estimate of the formation storativity. Papadopulos and Cooper (1967) showed that a plot of the logarithm of drawdown versus the logarithm of time provides a diagnostic test for borehole storage; borehole storage is characterized by the early-time unit slope on the log–log plot (Fig. 1b).

To estimate formation storativity from single-well tests where borehole storage is significant, it is necessary to examine the early-time drawdown. In step-drawdown tests, such information usually is ignored because the magnitude of the turbulent head losses calculated for a given pumping rate by the methods of Jacob (1947) or Rorabaugh (1953) are not necessarily constant at the onset of pumping. In this paper a mathematical model is developed for the early-time responses in pumped wells subject to both borehole storage and turbulent head losses, and a solution is derived to estimate formation properties. Because pumped wells may also be subject to formation damage or stimulation due to drilling practices, this paper also examines the effect of a borehole skin on the estimation of formation properties from single-well tests in wells subject to turbulent head losses. The results of these analyses are applied in estimating formation properties from a single-well test conducted in the Madison limestone near Rapid City, SD.

2. Transient response to turbulent head loss in a pumped well

Head losses in the vicinity of a pumped well are the result of several factors which may include losses across the well screen and fill material at the well screen, formation damage or stimulation due to drilling, turbulent flow in the formation near the well, and turbulent flow in the well itself (see, for example, Kruseman and de Ridder, 1991). Turbulent head losses in the well give rise to a discontinuity between the water level in the well and the piezometric surface in the formation at the well screen (Fig. 2). In this analysis we consider a well that is pumped at a constant rate and is subject to turbulent head losses. Because we are interested in examining the early-time responses in the pumped well and there may be a finite time needed for the pump to achieve a prescribed discharge rate at the onset of pumping, in this analysis we consider the recovering water level rather than the drawdown during pumping, and assume that turbulent head losses in the pumped well dissipate immediately when pumping is terminated. The turbulent head losses due to the pump operation will cease immediately when pumping ends; however, water from the formation will continue to flow into the borehole. Thus, we assume that the turbulent head loss

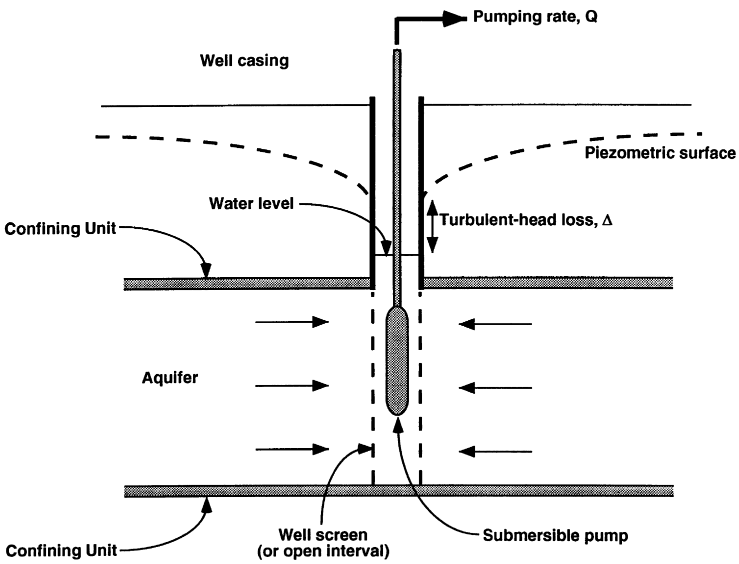

Fig. 2. Diagram of turbulent head loss in a pumped well and the hydraulic head in the surrounding formation.

from water flowing into the borehole is negligible during recovery. This, of course, is an assumption for the purpose of analyzing recovery data and estimating formation properties. The robustness of this assumption will be tested through comparison of model results with data from a field test.

At the onset of recovery, the discontinuity between the water level in the pumped well and the hydraulic head in the formation can be thought of as being analogous to the removal of a slug of water from the well at the instant pumping is terminated (Fig. 2). Thus, the water-level in the pumped well during recovery can be described by the following expression,

$$w(t)=H+h(r_s,t)-h(r_s,t-t_r)-g(r_s,t-t_r), \quad t \geq t_r \tag{1}$$

where t is time, t_r is the duration of pumping, w is the water level in the pumped well measured above an assumed datum, $h(r_s,t)$ and $h(r_s,t - t_r)$ are the hydraulic heads at the well screen due to pumping at a constant rate Q starting at time $t = 0$ and $t = t - t_r$, respectively, $g(r_s,t - t_r)$ is the drawdown at time $t - t_r$ that would be induced by removing a slug of water from the well (where the height of the slug is equal to the magnitude of the head losses), H is the ambient hydraulic head measured above an assumed datum and r_s is the radius of the well screen.

For the purpose of this analysis, we consider the recovering water level relative to the water level in the pumped well at $t = t_r$,

$$\rho(t)=w(t)-w(t_r)=w(t)-[h(r_s,t_r)-\Delta] \quad t \geq t_r \tag{2}$$

where $\rho(t)$ is the recovering water level relative to the water level at $t = t_r$, and Δ is the magnitude of the turbulent head loss. Using Eq. (1), $\rho(t)$ can be written

$$\begin{aligned}\rho(t)=w(t)-w(t_r)=H+h(r_s,t)-h(r_s,t-t_r)\\ -g(r_s,t-t_r)-[h(r_s,t_r)-\Delta] \quad t \geq t_r\end{aligned} \tag{3}$$

For simplicity we assume that pumping has been conducted for sufficient time such that $h(r_s,t)$ essentially remains unchanged for $t > t_r$. Thus, Eq. (3) can be reduced to

$$\zeta(t)=H-\rho(t)+\Delta=h(r_s,t-t_r)+g(r_s,t-t_r) \quad t \geq t_r \tag{4}$$

Because we are interested in analyzing the early-time recovery data following pumping, the hydraulic head at the well screen due to pumping, $h(r_s,t)$, does not necessarily have to be constant for $t > t_r$. Eq. (4) is appropriate if the duration of pumping is long relative to the time over which the recovery data is analyzed.

Because the right-hand side of Eq. (4) is only a function of $t - t_r$, then $\rho(t)$ also is only a function of $t - t_r$ and, thus, we can use $\tau = t - t_r$ and rewrite Eq. (4) as

$$\zeta(\tau)=H-\rho(\tau)+\Delta=h(r_s,\tau)+g(r_s,\tau) \quad \tau \geq 0 \tag{5}$$

In the above equation, $\zeta(\tau)$ is the superposition of the effects of pumping from a well and adding a slug of water to the well at the onset of pumping; the recovering water level, $\rho(\tau)$, is defined in terms of $\zeta(\tau)$.

3. Type curves and estimating storativity

To illustrate the effect of head loss on the recovering water-level in the pumped well, we consider a formation that is assumed to be confined, homogeneous, isotropic, of uniform thickness and infinite areal extent, and a finite diameter well with a well screen that fully penetrates the formation. For these conditions, the solution for $h(r_s,t)$ is given by Papadopulos and Cooper (1967) and $g(r_s,t)$ is the solution for applying a slug of water to a well given by Cooper et al. (1967). Fig. 3 shows a plot of the logarithm of the dimensionless form of $\rho(\tau)$ versus the logarithm of dimensionless time, where the dimensionless quantities are defined as

$$\rho' = \frac{4\pi T\rho}{Q} = \zeta' + \beta \tag{6}$$

$$t' = \frac{T\tau}{Sr_s^2} \tag{7}$$

$$\alpha = \frac{Sr_s^2}{r_c^2} \tag{8}$$

$$\beta = \frac{4\pi T\Delta}{Q} \tag{9}$$

$$\zeta' = \frac{4\pi T(h-\zeta)}{Q} \tag{10}$$

In Eq. (6), Eq. (7), Eq. (8), Eq. (9) and Eq. (10), ρ' is the dimensionless recovering water level in the

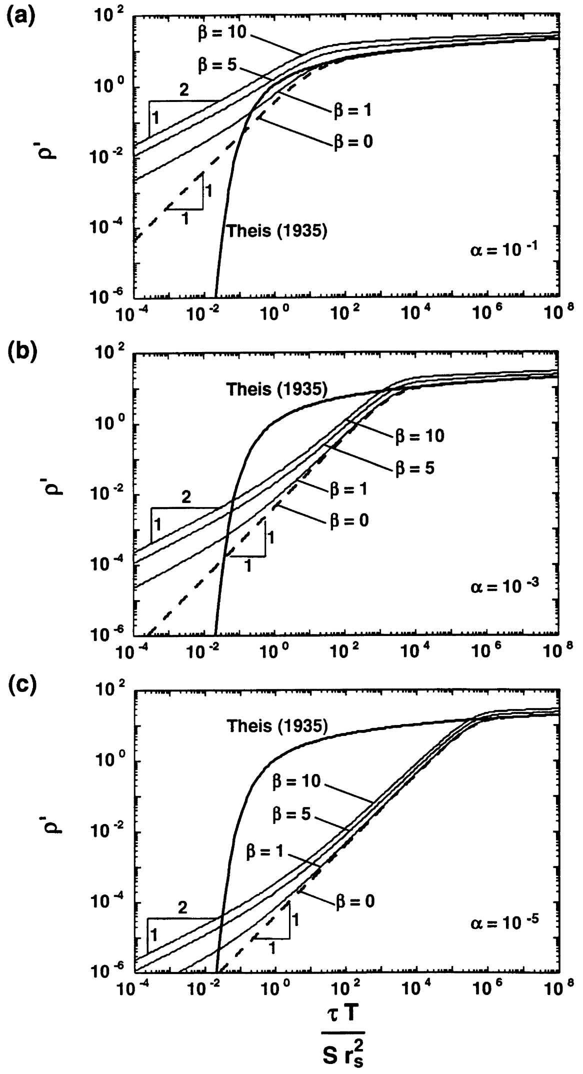

Fig. 3. Dimensionless recovering water level versus dimensionless time in a pumped well that has been subject to turbulent head loss during pumping.

pumped well, t' is the dimensionless time, α is the ratio of volumetric storage in the formation to volumetric storage in the borehole, β is the dimensionless magnitude of the head loss for the prescribed pumping rate, T is transmissivity, S is storativity, ζ' is the dimensionless form of ζ, and r_s and r_c are the radii of the screened (or open) interval of the well and the well casing, respectively.

For turbulent head loss in the pumped well, $\beta > 0$, the early-time recovery shows a slope of 1/2 on log–log plots of ρ' versus t' (Fig. 3). For smaller values of α, the log–log plots of ρ' versus t' gradually assume a unit slope as time increases, signifying the effect of borehole storage. This is followed by water-level responses in the pumped well that are representative of the formation responses. The half-slope response is most pronounced for larger values of α, and for $\alpha = 0.1$ the recovery due to head loss completely masks the effect of borehole storage. In Fig. 3, these results are compared with the solution of Theis (1935) for pumping from a well having an infinitesimal borehole diameter and, thus, instantaneous formation responses in the pumped well.

Characteristic curves similar to those in Fig. 3 can be used to estimate formation storativity in conjunction with the analysis of a step-drawdown test. For example, a step-drawdown test can be conducted to estimate the magnitude of the turbulent head loss, Δ, at the final pumping rate. Also, the formation transmissivity, T, can be estimated from the first step of the test using the method of Jacob (1947), provided that pumping has been conducted for sufficient time during the first step to observe the linear response on a semi-log plot of drawdown versus time. With the estimates of T and Δ, β is defined from Eq. (9), and type curves for ρ' for various values of α can be generated. An estimate of α can be obtained from fitting the type curves to the measured recovery data using standard methods of matching data and type curves (see, for example, Lohman, 1979). The formation storativity, S, is then determined from Eq. (8).

The half-slope response on log–log plots of recovery versus time arising from head losses in the pumped well can exist in other aquifer models. For other aquifer models, however, the solution for the recovering water-level cannot be developed by using the slug test solution of Cooper et al. (1967); a solution for a slug test in the type of aquifer under consideration would have to be used. In a subsequent section, a solution for a dual-porosity model is developed to interpret a single-well test conducted in a fractured limestone aquifer. Furthermore, the half-slope response on log–log plots of recovery versus time discussed above should not be confused with half-slope responses noted in other aquifer test solutions. For example, in fractured rock aquifers, a single fracture or highly permeable zone intersecting the pumped well can yield a linear flow regime which results in a half-slope response on log–log plots of drawdown versus time (Gringarten et al., 1974; Karasaki et al., 1988). The half-slope response discussed in this article is a borehole phenomenon and not a phenomenon associated with the formation.

4. Turbulent head losses and borehole skin

Using the value of α to estimate S from Eq. (8) assumes that r_s is known. However, if there is formation damage or stimulation resulting in a borehole skin, using the drilled or screened radius of the borehole may yield erroneous estimates of S from Eq. (8). Formation damage or stimulation in the vicinity of the borehole may produce a borehole skin with hydraulic properties different from those of the formation (Ramey, 1982). The interpretation of the recovering water level discussed above, however, assumes homogeneous aquifer properties.

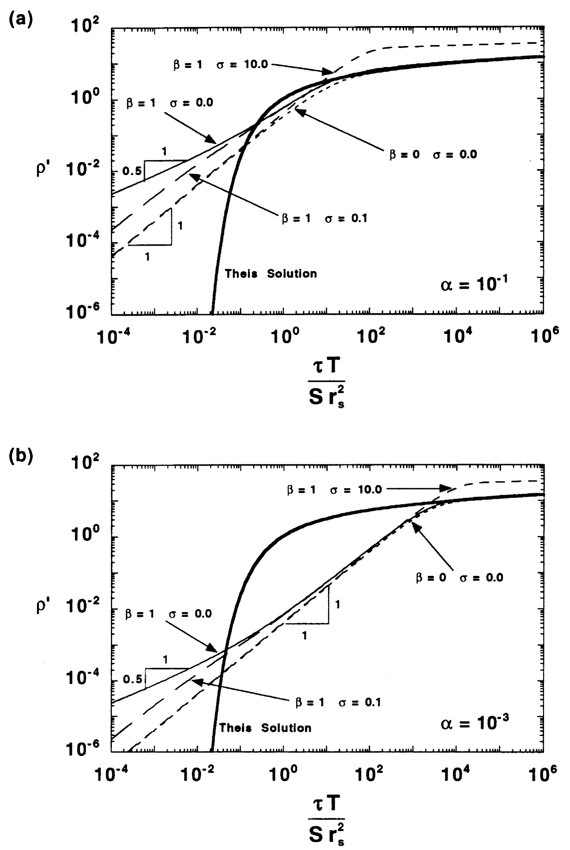

Fig. 4. Recovery versus time in a pumped well subject to borehole storage, turbulent head loss and borehole skin.

A finite thickness borehole skin can affect the early-time recovering water level in a pumped well that is subject to both borehole storage and turbulent head losses. Fig. 4 shows the effect on the recovering water level in the pumped well arising from a finite thickness borehole skin with no storativity, where σ is the dimensionless borehole skin factor, which is a constant relating the flux of water through the skin to the head difference across the skin. Moench and Hsieh (1985) show that a finite thickness borehole skin with no storativity has a skin factor equal to

$$\sigma = \frac{T}{T_{sk}} \ln\left(\frac{r_{sk}}{r_s}\right) \tag{11}$$

where r_{sk} is the radius of the skin and T_{sk} is the transmissivity of the skin. Formation stimulation is associated with cases where $T_{sk} > T$, and formation damage is associated with cases where $T_{sk} < T$. For $\sigma > 0$, there is a finite conductivity borehole skin with a linear head loss from the radius of the skin to the drilled or screened radius of the borehole. As σ approaches zero, the borehole skin becomes infinitely conductive with no head loss across the skin. The governing equations and the Laplace transform solution for the results given in Fig. 4 are developed in Appendix A.

Nonzero values of σ change the early-time slope of log–log plots of recovery versus time in pumped wells subject to turbulent head losses. As σ increases, the early-time slope on log–log plots of recovery versus time approaches unity, which is the same slope associated with the influence of borehole storage. Consequently, there is not a unique diagnostic shape for the time-varying response in a pumped well that will identify the presence of a borehole skin. Furthermore, the magnitude of the recovery at late-time is greater for cases in which $\sigma > 0$ than for cases in which $\sigma = 0$, because of the increased drawdown arising from the borehole skin. Because the presence of the borehole skin is difficult to identify, there is the danger that the value of α could be incorrectly estimated from type-curve matching with a model of a homogeneous formation.

One approach to identifying the presence of formation damage or stimulation in the vicinity of the borehole is discussed by Jacob (1947), who noted that if an estimate of S from an observation well is available, then the ‘effective’ radius of the pumped well can be estimated using the model that assumes a homogeneous formation. The ‘effective’ radius is defined as the radius of an undamaged well that gives the same measured drawdown as in the damaged well (Streltsova, 1988). Jacob (1947), however, proposed to identify the effective radius from the semilogarithmic plot of drawdown versus time. As noted earlier, for cases in which there is borehole storage, in a well subject to turbulent head losses, the use of the semilogarithmic plot for estimating S (and also the effective radius) will yield erroneous results.

The analysis in this paper for estimating the storage coefficient in wells subject to turbulent head losses considers early-time fluid responses in the pumped well and, therefore, provides a more accurate means of estimating the formation storativity than the late-time fluid responses in the pumped well. With the approach presented in this paper, the method proposed by Jacob (1947) for estimating the ‘effective’ radius of the pumped well could then be applied to identify the presence of formation damage or stimulation. For example, using type curves similar to those shown in Fig. 3 in which there is assumed to be no formation damage ($\sigma = 0$), a value of α can be estimated from type-curve matching to the measured recovery data. With an estimated value of S from an observation well or other information, Eq. (8) can be used to estimate the effective radius of the pumped well. An effective radius greater than the drilled or screened radius of the pumped well would imply formation stimulation, whereas an effective radius less than the drilled or screened radius of the borehole would imply formation damage.

5. Field application

To demonstrate the estimation of formation properties from single-well tests subject to borehole storage and turbulent head losses, a step-drawdown test was conducted in well RC7, which is completed in the Madison limestone in Rapid City, South Dakota. The test was conducted as part of a US Geological Survey investigation of the hydrogeology of the Madison aquifer near Rapid City, South Dakota

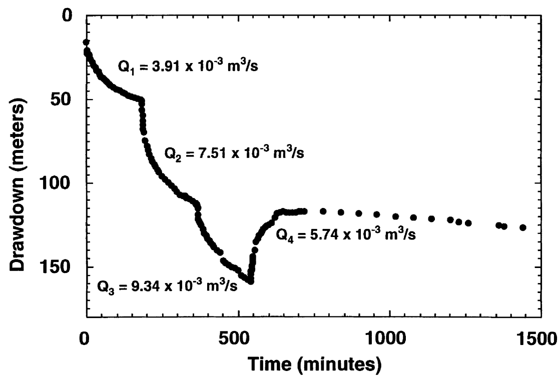

Fig. 5. Drawdown versus time in well RC7 during step-drawdown test.

(Greene, 1993). The well is cased with steel through the overlying formations and is completed as an open hole in the Madison limestone. The total depth of RC7 is 1000 m, and the open interval of the well begins at 851 m below land surface; however, only the upper 57 m of the open interval is fractured and produces water. The radius of the casing is 0.17 m and the drilled radius of the open interval is 0.16 m. However, the radius of the open interval varies significantly due to fracturing and acidizing that was conducted to increase the productivity of the well prior to testing.

The step-drawdown test was conducted in RC7 using four steps, in which a constant pumping rate was maintained during each step. The first three steps of the test were maintained for 3 h each, and the final step of the test was maintained for 15 h. At the end of the final step, the pump was turned off and recovery in the pumped well was monitored. A plot of drawdown versus time during the step-drawdown test

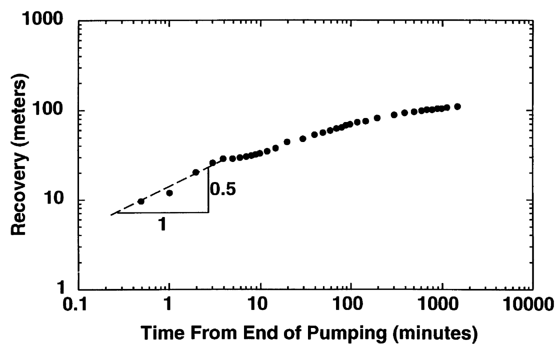

Fig. 6. Recovering water level versus time in well RC7 following the step-drawdown test.

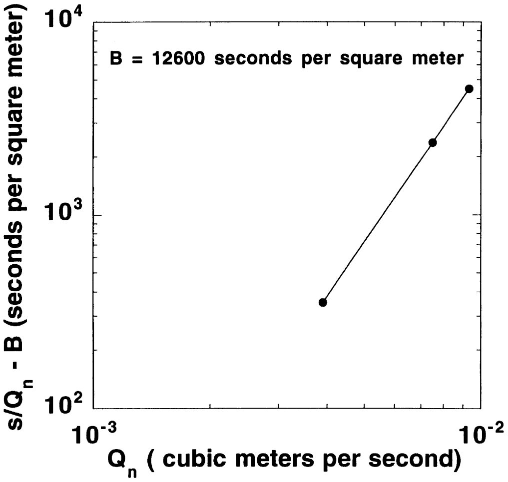

Fig. 7. Specific drawdown versus pumping rate for step-drawdown test in well RC7.

is shown in Fig. 5 and the recovery following pumping is shown in Fig. 6.

From the pumping rates and drawdown shown in Fig. 5, the method of Rorabaugh (1953) is used to estimate the head loss. Rorabaugh (1953) assumed that drawdown in a well subject to head losses is defined as

$$s = BQ + CQ^P \tag{12}$$

where s is the drawdown, Q is pumping rate, B is the coefficient associated with linear head losses and drawdown attributed to the formation, and C and P are coefficients associated with turbulent head losses. Fig. 7 shows a plot of the logarithm of $s/Q_n - B$ versus the logarithm of Q_n, where Q_n is the pumping rate for a given step of the test. From trial and error, B is defined as the value that gives a straight line in Fig. 7 (Rorabaugh, 1953). The slope of the straight line in Fig. 7 is equal to $P - 1$ and C is determined from the intercept of the straight line with $Q_n = 1$. From the results in Fig. 7, $B = 12\,600\ \mathrm{s/m^2}$, $P = 3.9$ and $C = 3.9 \times 10^9\ \mathrm{s^{3.9}/m^{10.7}}$. Using the values of B, C and P in Eq. (12), the turbulent head loss at the final pumping rate for the test in RC7 constitutes approximately 9% of the total drawdown, or 11.3 m. Thus, the recovering water level in the pumped well should be influenced by the turbulent head loss during pumping. Furthermore, because the final step of the step-drawdown test was conducted for 15 h, we assume that the assumptions leading to Eq. (5) are appropriate in analyzing the early-time recovery.

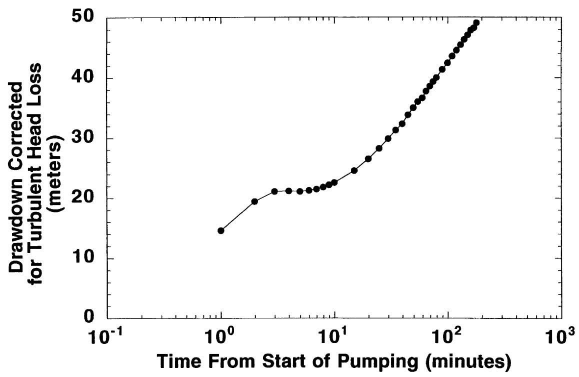

Fig. 8. Drawdown correct for turbulent head loss versus time during the first step of the step-drawdown test conducted in well RC7.

The water level in RC7 measured during the recovery part of the aquifer test (Fig. 6) illustrates a behavior that may be indicative of a dual-porosity medium. Because the well was acidized prior to aquifer testing, other conceptual models which consider heterogeneous formation properties also could be hypothesized, for example, the models of Barker and Herbert (1982) and Butler (1988). A similar dual-porosity response is also illustrated in the drawdown during the first step of the step-drawdown test. Fig. 8 shows the drawdown measured during the first step of the test, where drawdown corrected for turbulent head losses is plotted versus the logarithm of time; the corrected drawdown is calculated by subtracting the turbulent head loss (evaluated at late-time) from all head measurements. From the slope of the late-time straight-line portion of the drawdown curve in Fig. 8, the formation transmissivity is estimated to be $2.9 \times 10^{-5}\ \mathrm{m^2/s}$ (see, for example, Kruseman and de Ridder, 1991).

The slope of the early-time drawdown in Fig. 8 is not parallel to the late-time drawdown response, indicating there may be an influence from borehole storage. In looking at the recovering water level in Fig. 6, the slope on the early-time log–log plot of recovery versus time is approximately 1/2. From Fig. 6, one could hypothesize that a high-permeability fracture intersects the well and is embedded in a dual-porosity formation. However, in the aquifer test conducted in RC7, the half-slope response at the onset of the recovery is most likely the result of the

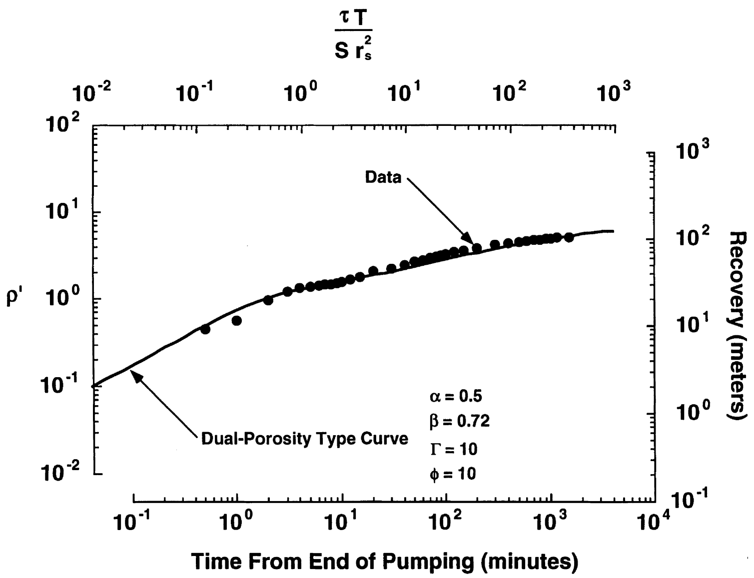

Fig. 9. Type-curve match between recovering water level versus time in well RC7 and a dual-porosity model of the formation assuming turbulent head loss in the pumped well.

turbulent-head loss in the pumped well which influences the early-time recovery.

Using type-curve solutions developed for a dual-porosity medium, which account for turbulent-head loss in the pumped well (see Appendix B), the storativity of the rock matrix, S_m, the storativity of the fractures, S, and the rate of fluid exchange between fractures and the rock matrix, γ, are determined from type-curve matching. The type curves are developed for $\beta = 0.72$, which uses the transmissivity estimated from the late-time response from the first step of the step-drawdown test and the magnitude of the turbulent head loss at the completion of pumping. The type curve that provides the best fit to the data is shown in Fig. 9, where $\alpha = 0.5$, $\Gamma = 10$ and $\phi = 10$; where α is defined by Eq. (8), and the dimensionless parameters Γ and ϕ are defined as

$$\Gamma = \frac{\gamma r_s^2}{T} \tag{13}$$

$$\phi = \frac{S_m}{S} \tag{14}$$

Using the value of $\alpha = 0.5$ from type-curve matching and the radius of the casing, $r_c = 0.17$ m, we obtain $Sr_s^2 = 1.4 \times 10^{-2}$ m^2 from Eq. (8). If the drilled radius of RC7 ($r_c = 0.16$ m) is used to estimate S, then we would obtain an unreasonably large estimate of fracture storativity. However, if we use a value of the storativity of the Madison limestone from a multiple-well aquifer test conducted in the vicinity of RC7, we can estimate the 'effective' radius of the pumped well and identify the effect of acidizing the well. The storativity of the Madison limestone from a multiple-well aquifer test analyzed by Greene (1993) was estimated to be 1×10^{-4}. This storativity was based on matching the late-time drawdown from observation wells using a single-porosity model of the Madison limestone; however, a break in slope in the early-time drawdown that could be attributable to a dual-porosity response was measured. Because the late-time drawdown from observation wells was used, the storativity estimated by Greene (1993) can be assumed to be the sum of the rock matrix storativity and the fracture storativity, $S_m + S = 1 \times 10^{-4}$. Using Eq. (14) and the value of $\phi = 10$ from type-curve matching in Fig. 9 we obtain $S = 9.0 \times 10^{-6}$ and $S_m = 9.1 \times 10^{-5}$. Using the value of S, the 'effective' radius of the pumped well is estimated from Eq. (8) to be 40 m. Furthermore, the remaining parameter of the dual-porosity model, γ, is estimated from Eq. (13). Using the 'effective' radius of the pumped well, γ is estimated to be 1.8×10^{-7} s^{-1}.

A value of 40 m for the 'effective' radius is indeed large relative to what would be expected in unconsolidated porous media; however, the 'effective' radius is an abstract measure of the heterogeneity in the vicinity of the borehole relative to what would be obtained if the formation was homogeneous. In highly heterogeneous fractured formations, large values of the 'effective' radius are conceivable and would arise due to both formation stimulation and the natural heterogeneity in the formation. In this case, it is plausible that both formation stimulation from acidizing the well and heterogeneity in the transmissivity in the vicinity of the well are contributing to the large 'effective' radius. It is unfortunate that the well was not tested prior to acidizing, in order to demonstrate the increase in the 'effective' radius due to acidizing. Furthermore, it must be recognized that there are many uncertainties in estimating the 'effective' radius, in particular, the estimate of storativity from a second well (or in this case, a totally independent aquifer test conducted in the vicinity) in a highly heterogeneous fractured rock terrane.

Because we have estimated an 'effective' radius of the pumped well, we must consider the presence of a borehole skin and its influence on the measured recovery. Because the early-time recovery in the pumped well shows a slope of 1/2 on the log–log plot of recovery versus time (Fig. 6), the borehole skin factor, σ, for RC7 must be relatively small, as large values of σ would force the recovery to assume a unit slope on log–log plots of recovery versus time (Fig. 4). Furthermore, the small value of σ implies that little of the total drawdown in the pumped well can be attributed to the resistance offered by the borehole skin.

6. Summary and conclusions

Estimating formation storativity from single-well tests often requires the analysis of early-time hydraulic responses in the pumped well. However, in pumped wells subject to turbulent head losses, the early-time data are frequently ignored because the turbulent head loss determined for a given pumping rate by the methods of Jacob (1947) or Rorabaugh (1953) is not necessarily constant at early time. Using the late-time data to estimate formation storativity may yield erroneous results, especially in wells that are also subject to borehole storage. In this paper, a mathematical model is developed for the early-time recovering water level following the termination of pumping from a step-drawdown test. The solution assumes that the turbulent head losses dissipate immediately when pumping ends. Although this is an approximation of the physical conditions encountered in the borehole, model results tend to correspond with recovery data measured during an aquifer test. Under this assumption, at the onset of recovery, the response in the pumped well is analogous to removing a slug of water from the pumped well at the instant pumping is terminated.

Type curves are developed from the mathematical model to estimate the formation storativity in a confined and homogeneous aquifer of constant thickness and infinite areal extent. The type curves show that in wells that are subject to both borehole storage and turbulent head losses, the early-time recovery exhibits a slope equal to 1/2 on a log–log plot of recovery versus time. The half-slope response would be measurable for larger values of the dimensionless storage coefficient, α, in particular, values of α greater than 10^{-3}. At later time, log–log plots of recovery versus time evolve to a unit slope which is indicative of borehole storage. This is then followed by water level responses in the pumped well that are representative of formation responses.

The solution for early time responses following pumping in a well subject to turbulent head losses can also be developed for other aquifer models. The solution for a dual-porosity aquifer is developed and used to analyze the results from a single-well test conducted in the Madison limestone near Rapid City, South Dakota. The measured recovery data showed an early-time half-slope response on a log–log plot of recovery versus time. Estimates of the fracture and rock matrix storativities were obtained from matching the type curves with the measured recovery data. The estimates of the storativities, however, appeared to be unreasonably large. Using an estimate of fracture storativity from other aquifer tests conducted in the same formation provided an estimate of the 'effective' radius of the pumped well. The 'effective' radius was larger than the drilled radius of the well, which is consistent with the formation stimulation that was conducted by acidizing the well prior to testing. The large 'effective' radius

(40 m) could also be an artifact of heterogeneity local to the pumped borehole.

For situations in which there is borehole damage or stimulation, a borehole skin can influence the early-time recovery of wells subject to turbulent head losses. The early-time response in wells with a borehole skin becomes similar to the response associated with borehole storage as the skin factor, σ, becomes larger. The fact that a half-slope response during recovery was measured in the test conducted in the Madison limestone indicates that the borehole skin had a relatively small skin factor.

Finally, caution must be used when hypothesizing aquifer characteristics and estimating aquifer properties, especially in circumstances where the shape of time-drawdown plots from aquifer tests can be explained by different conceptual models of the aquifer. In this investigation, a solution is developed which shows that the recovering water level in a pumped well that is subject to turbulent-head loss has a slope equal to 1/2 on a log–log plot of recovery versus time. An early-time half-slope response also is characteristic of a linear-flow regime, which may be caused by a single fracture or a high-permeability zone intersecting the pumped well.

The single-well test conducted in the Madison limestone in Rapid City, South Dakota, exhibited a half-slope response at the onset of recovery. A step-drawdown test in the same well illustrated that the pumped well was subject to turbulent-head loss during pumping. The half-slope response could have been hypothesized as a linear flow regime due to a high-permeability zone intersecting the well. Instead, the analysis presented in this article showed that the half-slope response can be attributed to a borehole phenomenon arising from the turbulent head losses in the pumped well. These results illustrate the importance of conducting step-drawdown tests as a precursor to identifying a conceptual model of the formation and formation properties from single-well tests.

Nomenclature

B	coefficient of linear head losses in a pumped well defined in Eq. (12)
C	coefficient of turbulent head losses in a pumped well defined in Eq. (12)
g	change in the hydraulic head induced by removing a slug of water equal to the magnitude of the head losses
h	hydraulic head in the formation or the hydraulic head in fractures
h_m	hydraulic head in the rock matrix
H	ambient hydraulic head in the formation
p	Laplace transform parameter
P	coefficient of turbulent head losses in a pumped well defined in Eq. (12)
Q	pumping rate
r	radial distance
r'	dimensionless form of r defined in Eq. (A8)
r_c	casing radius
r_s	radius of screened or open interval of the pumped well
r_{sk}	radius of the borehole skin
s	drawdown
s'	dimensionless form of h defined in Eq. (A7)
$\overline{s'}$	Laplace transform of s'
$s_m{}'$	dimensionless form of h_m defined in Eq. (B9)
$\overline{s_m{}'}$	Laplace transform of $s_m{}'$
S	formation storativity or fracture storativity
S_m	rock matrix storativity
t	time
t'	dimensionless form of τ
t_r	duration of pumping
T	formation transmissivity or fracture transmissivity
T_{sk}	transmissivity of the borehole skin
w	water level in the pumped well
α	dimensionless storage coefficient defined in Eq. (8)
β	dimensionless turbulent head loss defined in Eq. (9)
γ	fluid exchange rate between fractures and rock matrix
Γ	dimensionless fluid exchange rate between fractures and rock matrix defined in Eq. (13)
Δ	magnitude of the turbulent head loss at the end of pumping
ϕ	ratio of storativity in the rock matrix to storativity in fractures
ρ	recovering water level relative to water level at $t = t_r$
σ	dimensionless borehole skin factor defined in Eq. (11)
ρ'	dimensionless form of ρ defined in Eq. (6)
τ	time since the end of pumping
ζ	superposition of the effects of pumping from a well and adding a slug of water to the well at the onset of pumping
ζ'	dimensionless form of ζ defined in Eq. (10)
$\overline{\zeta'}$	Laplace transform of ζ'

Appendix A

The discussion and assumptions leading to Eq. (5) show that the recovering water level in a well subject to turbulent head losses is analogous to applying an instantaneous slug of water to the pumped well at the onset of pumping. In the following, a Laplace transform solution for $\zeta(\tau)$ is developed for the case of a confined, homogeneous and isotropic formation of infinite areal extent, where the pumped well fully penetrates the formation and a finite thickness borehole skin with no storativity surrounds the pumped well. From the solution for $\zeta(\tau)$, the recovering water level in a well subject to head losses, $\rho(\tau)$, is defined from Eq. (5).

For the conditions discussed above, the water level in the pumped well is defined as

$$\zeta(\tau)=\left(h(r,\tau)-r\sigma\,\frac{\partial h}{\partial r}\right)\Big|_{r=r_{sk}} \tag{A1}$$

which is subject to the initial condition

$$\zeta(\tau=0)=H+\Delta \tag{A2}$$

The terms used in these equations, and those that follow, are defined in the Nomenclature section.

To define the water level in the pumped well, the hydraulic head in the formation, h, must be defined from the equations governing fluid movement in the formation,

$$S\,\frac{\partial h}{\partial \tau}-T\,\frac{1}{r}\frac{\partial}{\partial r}\left(r\,\frac{\partial h}{\partial r}\right)=0 \tag{A3}$$

Eq. (A3) is subject to the initial condition,

$$h(r,\tau=0)=H \tag{A4}$$

and the boundary conditions,

$$-\pi r_c^2\,\frac{d\zeta}{d\tau}+\left(2\pi rT\,\frac{\partial h}{\partial r}\right)\Big|_{r=r_{sk}}=Q \tag{A5}$$

$$h(r\rightarrow\infty,\tau)=H \tag{A6}$$

In the following, we make use of the following dimensionless variables, as well as those defined in Eq. (7), Eq. (8), Eq. (9) and Eq. (10),

$$s'=\frac{4\pi T(H-h)}{Q} \tag{A7}$$

$$r'=\frac{r}{r_s} \tag{A8}$$

Introducing Eq. (7), Eq. (8), Eq. (9) and Eq. (10), and Eq. (A1)–(A6) yields

$$\zeta'(t')=\left(s'(r',t')-r'\sigma\,\frac{\partial s'}{\partial r'}\right)\Big|_{r'=\frac{r_{sk}}{r_s}} \tag{A9}$$

$$\zeta'(t'=0)=-\beta \tag{A10}$$

$$\frac{\partial s'}{\partial t'}-\frac{1}{r}\frac{\partial}{\partial r'}\left(r'\,\frac{\partial s'}{\partial r'}\right)=0 \tag{A11}$$

$$s'(r',t'=0)=0 \tag{A12}$$

$$\frac{1}{2\alpha}\frac{d\zeta'}{dt'}-\left(r'\,\frac{\partial s'}{\partial r'}\right)\Big|_{r'=\frac{r_{sk}}{r_s}}=2 \tag{A13}$$

$$s'(r'\rightarrow\infty,t')=0 \tag{A14}$$

where α and β are defined in Eq. (8) and Eq. (9), respectively.

Taking the Laplace transform of Eq. (A9)–(A14) yields

$$\overline{\zeta'}=\left(s'(r')-r'\sigma\,\frac{\partial\overline{s'}}{\partial r'}\right)\Big|_{r'=\frac{r_{sk}}{r_s}} \tag{A15}$$

$$p\overline{s'}-\frac{1}{r'}\frac{\partial}{\partial r'}\left(r'\,\frac{\partial\overline{s'}}{\partial r'}\right)=0 \tag{A16}$$

$$\frac{1}{2\alpha}(p\overline{\zeta'}+\beta)-\left(r'\,\frac{\partial\overline{s'}}{\partial r'}\right)\Big|_{r'=\frac{r_{sk}}{r_s}}=\frac{2}{p} \tag{A17}$$

$$\overline{s'}(r'\rightarrow\infty)=0 \tag{A18}$$

where p is the Laplace transform variable, and $\overline{s'}$ and $\overline{\zeta'}$ are the Laplace transforms of s' and ζ', respectively.

From Eq. (A15)–(A18), the solution for $\overline{s'}$ is

$$\overline{s'}(r')=\frac{(4\alpha-\beta p)K_0(r'\sqrt{p})}{p[pK_0(\eta)+(2\alpha+\sigma p)\eta K_1(\eta)]} \tag{A19}$$

and the solution for $\overline{\zeta'}$ is

$$\overline{\zeta'}=\frac{(4\alpha-\beta p)[K_0(\eta)+\eta\sigma K_1(\eta)]}{p[pK_0(\eta)+(2\alpha+\sigma p)\eta K_1(\eta)]} \tag{A20}$$

where

$$\eta=\frac{r_{sk}}{r_s}\sqrt{p}.$$

The solutions for s' and ζ' can be evaluated from Eq. (A19) and Eq. (A20), respectively, by numerically inverting the Laplace transform (see, for example, Stehfest, 1970).

Appendix B

The discussion and assumptions leading to Eq. (5) also are applicable to various conceptual models of an aquifer. In the following, the recovering water level in a pumped well subject to turbulent head loss in a dual-porosity medium is developed. Similar to the development in Appendix A, a Laplace transform solution for $\zeta(\tau)$ is developed from which the recovering water level in the pumped well, $\rho(\tau)$, is defined from Eq. (5). In this analysis, we consider a confined, homogeneous and isotropic formation of infinite areal extent, where the pumped well fully penetrates the formation; however, there is assumed to be no borehole skin at the pumped well.

For the conditions discussed above, the water level in the pumped well is defined as

$$\zeta(\tau)=h(r=r_{\mathrm{s}},\tau) \tag{B1}$$

which is subject to the initial condition

$$\zeta(\tau=0)=H+\Delta \tag{B2}$$

The terms used in these equations, and those that follow, are defined in the Nomenclature section.

To define the water level in the pumped well, the hydraulic head in the fractures, h, is defined from the equations governing fluid movement in a dual-porosity medium, where the equation governing fluid movement in fractures is (Barenblatt et al., 1960)

$$S\ \frac{\partial h}{\partial \tau}-T\ \frac{1}{r}\frac{\partial}{\partial r}\left(r\ \frac{\partial h}{\partial r}\right)=\gamma(h_{\mathrm{m}}-h) \tag{B3}$$

and the equation for flow in the rock matrix is

$$S_{\mathrm{m}}\ \frac{\partial h_{\mathrm{m}}}{\partial \tau}=-\gamma(h_{\mathrm{m}}-h) \tag{B4}$$

The initial conditions for Eq. (B3) and Eq. (B4) are

$$h(r,\tau=0)=H \tag{B5}$$

$$h_{\mathrm{m}}(\tau=0)=H \tag{B6}$$

The boundary conditions for Eq. (B3) are

$$-\pi r_{\mathrm{c}}^{2}\ \frac{\mathrm{d}\zeta}{\mathrm{d}\tau}+\left(2\pi rT\ \frac{\partial h}{\partial r}\right)\Big|_{r=r_{\mathrm{sk}}}=Q \tag{B7}$$

$$h(r\rightarrow\infty,\tau)=H \tag{B8}$$

In the following, we make use of dimensionless variables defined in Eq. (7), Eq. (8), Eq. (9) and Eq. (10), and Eq. (A7) and Eq. (A8), along with the dimensionless form of s_{m},

$$s_{\mathrm{m}}{}'=\frac{4\pi T(H-h_{\mathrm{m}})}{Q} \tag{B9}$$

Introducing Eq. (7), Eq. (8), Eq. (9) and Eq. (10), and Eq. (A7), Eq. (A8) and Eq. (A9) into Eq. (B1)–(B8) yields

$$\zeta'(t')=s'(r'=1,t') \tag{B10}$$

$$\zeta'(t'=0)=-\beta \tag{B11}$$

$$\frac{\partial s'}{\partial t'}-\frac{1}{r}'\frac{\partial}{\partial r'}\left(r'\ \frac{\partial s'}{\partial r'}\right)=\Gamma(s_{\mathrm{m}}{}'-s') \tag{B12}$$

$$\phi\ \frac{\partial s_{\mathrm{m}}{}'}{\partial t'}=-\Gamma(s_{\mathrm{m}}{}'-s') \tag{B13}$$

$$s'(r',t'=0)=0 \tag{B14}$$

$$s_{\mathrm{m}}{}'(t'=0)=0 \tag{B15}$$

$$\frac{1}{2\alpha}\frac{\mathrm{d}\zeta'}{\mathrm{d}t'}-\frac{\partial s'}{\partial r'}\Big|_{r'=1}=2 \tag{B16}$$

$$s'(r'\rightarrow\infty,t')=0 \tag{B17}$$

where α and β are defined by Eq. (8) and Eq. (9), respectively, and Γ and ϕ are defined by Eq. (13) and Eq. (14), respectively.

Taking the Laplace transform of Eq. (B10)–(B17) yields

$$\overline{\zeta'}=\overline{s'}(r'=1) \tag{B18}$$

$$p\overline{s'}-\frac{1}{r'}\frac{\partial}{\partial r'}\left(r'\ \frac{\partial\overline{s'}}{\partial r'}\right)=\Gamma(\overline{s_{\mathrm{m}}{}'}-\overline{s'}) \tag{B19}$$

$$\overline{s_{\mathrm{m}}{}'}=\frac{\Gamma}{p\phi+\Gamma}\ \overline{s'} \tag{B20}$$

$$\frac{1}{2\alpha}(p\overline{\zeta'}+\beta)-\frac{\partial\overline{s'}}{\partial r'}|_{r'=1}=\frac{2}{p} \tag{B21}$$

$$\overline{s'}(r'\rightarrow\infty)=0 \tag{B22}$$

From Eq. (B18)–(B22), the solution for $\overline{s'}$ is

$$\overline{s'}(r')=\frac{(4\alpha-\beta p)K_0(r'\xi)}{p[pK_0(\xi)+2\alpha\xi K_1(\xi)]} \tag{B23}$$

and the solution for $\overline{\zeta'}$ is

$$\overline{\zeta'}=\frac{(4\alpha-\beta p)K_0(\xi)}{p[pK_0(\xi)+2\alpha\xi K_1(\xi)]} \tag{B24}$$

where

$$\xi=\sqrt{p+\frac{p\phi\Gamma}{p\phi+\Gamma}}.$$

The solutions for s' and ζ' can be evaluated from Eq. (B23) and Eq. (B24), respectively, by numerically inverting the Laplace transform (see, for example, Stehfest, 1970).

References

Barenblatt, G.I., Zheltov, Iu.P., Kochina, I.N., 1960. Basic concepts in the theory of seepage of homogeneous liquids in fissured rocks, J. Appl. Mathematics Mechanics (English Translation), 24, 1286–1303.

Barker, J.A., Herbert, R., 1982. Pumping tests in patchy aquifers, Ground Water, 20 (2), 150–155.

Butler, J.J., 1988. Pumping tests in nonuniform aquifers—The radially symmetric case, J. Hydrol., 101, 15–30.

Cooper, H.H., Bredehoeft, J.D., Papadopulos, I.S., 1967. Response of a finite-diameter well to an instantaneous charge of water, Water Resources Res., 3 (1), 263–269.

Greene, E.A., 1993. Hydraulic properties of the Madison aquifer system in the western Rapid City area, South Dakota. US Geological Survey Water-Resources Investigations Report 93-4008, 56 pp.

Gringarten, A.C., Ramey, H.J., Raghavan, R., 1974. Unsteady-state pressure distributions created by a well with a single infinite-conductivity vertical fracture, Soc. Petroleum Engineers J., 14, 347–360.

Jacob, C.E., 1947. Drawdown test to determine effective radius of artesian well, Trans. Am. Soc. Civil Engineers, 112, 1047–1070.

Karasaki, K., Long, J.C.S., Witherspoon, P.A., 1988. Analytical models of slug tests, Water Resources Res., 24 (1), 115–126.

Kruseman, G.P., de Ridder, N.A., 1991. Analysis and Evaluation of Pumping Test Data, 2nd ed., Publication 47, International Institute for Land Reclamation and Improvement. Wageningen, The Netherlands, 377 pp.

Lohman, S.W., 1979. Ground-water hydraulics. US Geological Survey Professional Paper 708, 70 pp.

Moench, A.F., Hsieh, P.A., 1985. Comment on ‘Evaluation of slug tests in wells containing a finite-thickness skin’, by Faust, C.R., Mercer, J.W., Water Resources Res., 21(9) 1459–1461.

Papadopulos, I.S., Cooper, H.H., 1967. Drawdown in a well of large diameter, Water Resources Res., 3 (1), 241–244.

Ramey, H.J., 1982. Well-loss function and the skin effect: A review. In: Recent Trends in Hydrogeology, Special Paper 189. Geological Society of America. Boulder, CO, pp. 265–271.

Rorabaugh, M.J., 1953. Graphical and theoretical analysis of step-drawdown test of artesian well, Proc. Am. Soc. Civil Engineers, 79 (Separate no. 362), 23 pp.

Stehfest, H., 1970. Algorithm 368—Numerical inversion of Laplace transforms, Communications Assoc. Computing Machinery, 13 (1), 47–49.

Streltsova, T.D., 1988. Well testing in heterogeneous formations. Wiley, New York, 413 pp.

Theis, C.V., 1935. The relation between the lowering of the piezometric surface and the rate and duration of discharge of a well using ground-water storage, Eos, Trans. Am. Geophys. Union, 16, 519–524.